Biosensors and Bioelectronics 156 (2020) 112134

Contents lists available at ScienceDirect

Biosensors and Bioelectronics

journal homepage: http://www.elsevier.com/locate/bios

Hierarchical 0D-2D bio-composite film based on enzyme-loaded polymeric nanoparticles decorating graphene nanosheets as a high-performance bio-sensing platform

Sheng Xu [a,b], Yayuan Liu [a], Wei Zhao [a], Qian Wu [a], Yanru Chen [a], Xuewen Huang [a], Zhijian Sun [b], Ye Zhu [a,**], Xiaoya Liu [a,*]

[a] Key Laboratory of Synthetic and Biological Colloids, Ministry of Education, School of Chemical and Material Engineering, Jiangnan University, Wuxi, 214122, Jiangsu Province, PR China

[b] School of Materials Science and Engineering, Georgia Institute of Technology, Atlanta, GA, 30332, United States

ARTICLE INFO

Keywords:
0D-2D nanocomposite film
Enzymatic biosensor
Graphene oxide
Electrophoretic deposition
H_2O_2 detection

ABSTRACT

Herein, we developed a hierarchical bio-composite sensing film by facile one-step electro-deposition of 0D enzyme-polymer nanoparticles (NPs) with 2D graphene oxide nanosheets as conductive supports and nanofillers, based on which an effective and robust enzymatic biosensor platform was constructed. Horseradish peroxidase (HRP) as a model enzyme was co-assembled with a photo-cross-linkable polypeptide of 2-hydroxyethyl methacrylate modified poly(γ-glutamic acid) (γ-PGA-HEMA), generating hybrid HRP@γ-PGA-HEMA nanoparticles (HRP@PGH NPs). Then HRP@PGH NPs and graphene oxide nanosheets (GO NSs) were simultaneously electrodeposited onto the electrode surface, obtaining a hierarchical 0D-2D bio-composite film. After subsequent electrochemical reduction of GO NSs into graphene nanosheets (GNSs) and following photo-cross-linking, the resultant nanostructured HRP@PGH/GNSs sensing film was successfully applied to construct an enzymatic biosensor for hydrogen peroxide (H_2O_2). The biosensor exerted high sensitivity, fast response, and good stability for H_2O_2 sensing. Satisfactory results were also demonstrated for its practical application in human serum samples, suggesting a promising application potential in biomedical diagnostics. The one-step generated 0D-2D bio-composite sensing film demonstrates synergetic effects from both the soft nanoparticles and hard conductive nanosheets, which would enlighten the innovative construction of composite nanomaterials and nano-architectonics for bio-sensing systems.

1. Introduction

Taking advantages of simple fabrication and operation, fast response, portability, integration et al., biosensors have aroused considerable interest from lab research to industrial applications in biomedical diagnosis, food security and environmental monitoring in recent decades (Das et al., 2016; Turner, 2013). Especially, enzymatic biosensor employing enzymes as recognition elements has been regarded as the most promising biosensor for industrialization and commercialization. Compared with other biosensors, enzymatic biosensor show ultrahigh specificity towards target molecules and enzymes could be generated at industrial levels (Yang, 2012). For an enzymatic biosensor, the key challenge lies in how to effectively immobilize the biological enzymes with molecular recognition ability on the biosensor surface. Though significant advance has been achieved for enzyme immobilization, these traditional methods often involve a tedious multi-step immobilization process, leading to damaged bioactivity of these biological enzymes and thus decreased sensing performance (Xu et al., 2019a). In addition, due to weak interactions between enzymes and support materials, undesired leakage of enzymes would occur over time, resulting in gradual deterioration in sensing performance (Lee et al., 2005). Therefore, it remains a significant challenge to pullulate more effective strategy as well as material in constructing enzymatic biosensor systems (Gerard et al., 2002; Lu et al., 2010).

Recently, graphene-based nanocomposites have demonstrated strong strengths in biosensors benefiting from the superior properties of

* Corresponding author.
** Corresponding author.
E-mail addresses: zhuye@jiangnan.edu.cn (Y. Zhu), lxy@jiangnan.edu.cn (X. Liu).

https://doi.org/10.1016/j.bios.2020.112134
Received 28 October 2019; Received in revised form 19 February 2020; Accepted 3 March 2020
Available online 6 March 2020

graphene, including high surface area, robust mechanical strength and high electrical conductivity (Justino et al., 2017; Liu et al., 2012; Ren et al., 2017a). In particular, graphene oxide (GO), an important derivative of graphene with 2D nanostructure, has been proven an ideal carbon-based material for enzyme immobilization in biological sensing platforms due to its high water dispersibility, biocompatibility, affinity for specific biomolecules, and comparable properties to graphene (Zhang and Chen, 2017). Recently, the integration of GO with polymers for multi-functional nanocomposites have attracted intense attention for enzyme immobilization in biosensor systems (Putzbach et al., 2013; Zhu et al., 2015). However, most polymer/GO nanocomposites are generally synthesized in bulk forms without obvious nanostructures, resulting in limited enzyme immobilization capacity. In addition, enzymes are deeply buried beneath the composite surface, leading to high mass transfer resistance between the active sites and target molecules and poor response sensitivity. In respect of above issues, it's highly envisioned that enhanced sensing performance would be realized if hierarchical nanostructures were incorporated in enzymatic biosensors by considering both the intrinsic properties and structural forms of the polymer/GO nanocomposite.

Herein, an effective "structure matters" strategy for fabricating enzymatic biosensor platform based on one-step electrodeposition of 0D hybrid enzyme-polymer nanoparticles (NPs) with 2D graphene oxide nanosheets as conductive nanofillers (Scheme 1) were demonstrated. By chemically conjugating 2-hydroxyethyl methacrylate (HEMA) with poly (γ-glutamic acid) (γ-PGA), a functionalized biopolymer (γ-PGA-HEMA) with photo-cross-linkable C═C bonds was synthesized first. Then, γ-PGA-HEMA was used as a polymer matrix to immobilize a model enzyme namely horseradish peroxidase (HRP) via co-assembly in aqueous solution, generating complex HRP@γ-PGA-HEMA nanoparticles (HRP@PGH NPs). To fabricate enzymatic biosensor, water-dispersed graphene oxide nanosheets (GO NSs) were co-deposited with HRP@PGH NPs on electrode surface by one-step electrophoretic deposition, obtaining a hierarchical 0D-2D bio-composite film (HRP@PGH/GO) with 0D enzyme-polymer NPs decorating 2D GO NSs. After electrochemical reduction of GO NSs into graphene nanosheets (GNSs) and following photo-cross-linking, an enzymatic biosensor was fabricated based on the formed HRP@PGH/GNSs bio-composite film. The photo-crosslinking among the polymeric NPs could not only prevent enzyme leakage but also enhance the structural stability of the integrated bio-composites, while the 2D GNSs could accelerate electron transfer across the sensing film. The hierarchical 0D-2D nanostructure exhibits synergetic strengths from the individual polymer nanoparticles and conductive carbon nanosheets, which is expected to render the developed biosensor with enhanced sensitivity, long-term stability and reliable practicability for real applications. In addition, one-step electrodeposition provides a cost-effective and controllable way to produce hierarchically nanostructured bio-composite film, which would definitely illuminate the creative generation of other bio-sensing systems and devices. The co-assembled HRP@PGH NPs as well as the bio-composite films have been systematically characterized. The overall performance of the 0D-2D HRP@PGH/GNSs film-based biosensor was also studied in detail. The excellent bio-sensing results related with the materials and structures are discussed below, revealing the advantageous potential of this highly effective strategy in biosensors and bioelectronics.

2. Experimental

All the reagents and materials, the preparation of complex enzyme-polymer nanoparticles (HRP@PGH NPs), the preparation of graphene oxide (GO), the fabrication of enzymatic biosensor, the detail characterization and measurement can be found in Supporting Information.

3. Results and discussion

3.1. Structural characterization of γ-PGA-HEMA

One key issue for an enzymatic biosensor is to effectively immobilize the recognition element on sensor electrode with improving these biomacromolecules' activity and stability. In this regard, the polymer carrier applied as bio-sensing material is required to show high compatibility with enzymes. γ-PGA, a naturally generated anionic polypeptide by microorganisms, has been widely applied in biomedical fields benefiting from its biodegradability and non-toxicity to humans and the environment (Sung et al., 2005; Xu et al., 2017). Thanks to the

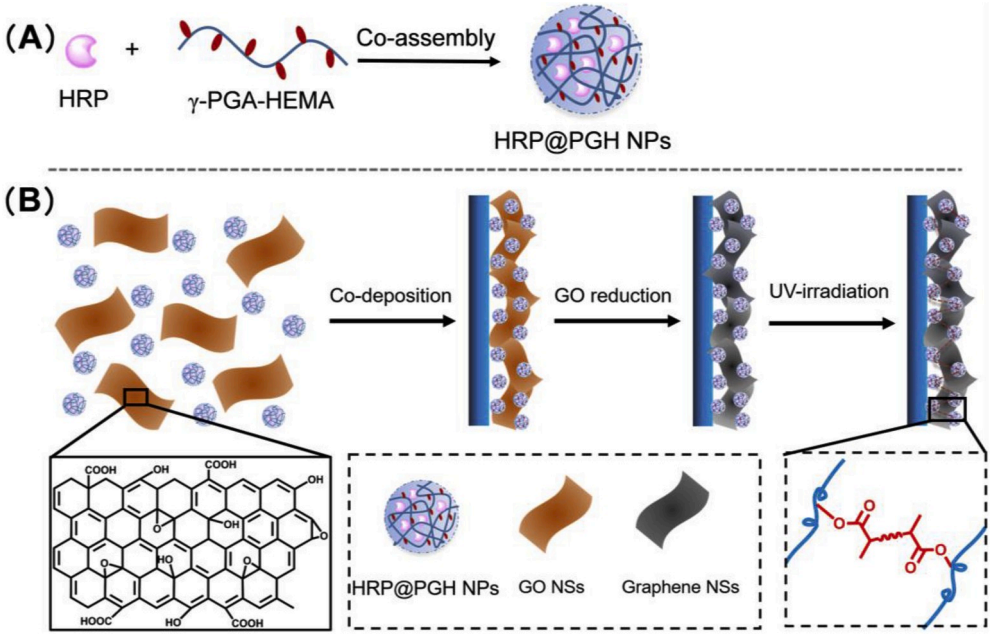

Scheme 1. Schematic illustration of the enzymatic biosensor based on bio-composite HRP@PGH/GNSs sensing film. (A) Preparation of enzyme-polymer nanoparticles HRP@PGH NPs via co-assembly of HRP and γ-PGA-HEMA. (B) Fabrication of the complex HRP@PGH/GNS sensing film via electrophoretic co-deposition of 0D HRP@PGH NPs and 2D graphene oxide (GO NSs).

existing carboxylic groups on γ-PGA side chains, a great deal of functional units could be incorporated into γ-PGA for enhanced functionalization. Herein, γ-PGA was endowed with photo-cross-linkable property by conjugating 2-hydroxyethyl methacrylate (HEMA) onto γ-PGA skeleton using EDC·HCl as coupling agent and DMAP as catalyst, respectively (Scheme S1). The biocompatibility of HEMA at the cell and tissue levels has been widely reported (Montheard et al., 1992), therefore the produced functional γ-PGA-HEMA biopolymer is expected to be a bio-compatible and solid support for enzyme immobilization in bio-sensing systems. The ^{1}H NMR spectra of γ-PGA and γ-PGA-HEMA are shown in Fig. S1, which confirms the successful synthesis of the photo-cross-linkable γ-PGA-HEMA biopolymer.

3.2. Characterization of enzyme-loaded HRP@PGH NPs

γ-PGA-HEMA has properties of a polypeptide due to its polypeptide molecular chain, therefore it is expected to exhibit high affinity when being used for enzyme immobilization in biosensors. To investigate the effectiveness of γ-PGA-HEMA in enzyme immobilization, horse radish peroxidase (HRP) was selected as a proof-of-concept model enzyme due to its high availability, low cost and high purity (Veitch, 2004). With heme acting as an active site and heme iron Fe(III) as a prosthetic group, HRP has been widely exploited in enzymatic H_2O_2 biosensors. In this work, the isoelectric point (pI) of HRP enzyme is around 8.8. As a result, HRP is positively charged in physiological environment, making it possible to interact with the negatively charged γ-PGA-HEMA. The zeta potential values of pure HRP and γ-PGA-HEMA in ultrapure water are -41.7 mV and 14.0 mV, respectively. Therefore, HRP enzymes were co-assembled with γ-PGA-HEMA in aqueous solution, resulting in the formation of water-compatible enzyme-polymer conjugates (zeta potential: -10.6 mV), as illustrated in Scheme 1A.

Fig. 1A shows the particle size and distribution of HRP@γ-PGA-HEMA conjugates by dynamic light scattering (DLS), indicating that nano-sized conjugates with an average hydrodynamic diameter of around 113 nm were formed during the co-assembly process. In addition, a small peak at around 3 nm could also be observed with very low intensity, which is attributed to the size distribution of free HRP enzymes in aqueous solution. Compared with pure γ-PGA-HEMA aggregates with a particle size of approximately 197 nm (Fig. S2), the deceased size after HRP incorporation indicates the formation of relatively compact nanocomposite due to interactions (hydrogen bond, electrostatic interaction, and et al.) between HRP and γ-PGA-HEMA. The morphological form of the enzyme-polymer conjugate is revealed in the TEM and AFM images of HRP@γ-PGA-HEMA (Fig. 1B and C). For comparisons, TEM and AFM images of pure γ-PGA and γ-PGA-HEMA were also provided in Fig. S3. As shown, γ-PGA exhibits continuous film morphology after drying from water, which is due to the chain entanglement of polymer chains from swelling coils after water evaporation. Unlike pure γ-PGA chains, γ-PGA-HEMA exhibits irregular aggregate morphology with wide size distribution. This is due to that the presence of HEMA on side chains changed the original solubility of γ-PGA in water, which makes the modified γ-PGA-HEMA become amphiphilic copolymer. Therefore, the γ-PGA-HEMA copolymers could self-assemble into nanoaggregates in water. It's worth noting that HEMA moieties are randomly distributed at the side chains of γ-PGA, as a result, γ-PGA-HEMA would behave like amphiphilic random copolymers in the self-assembly process. Therefore, the assembled γ-PGA-HEMA aggregates show wider size distribution in line with random copolymers than these regular copolymers like block copolymers. In the presence of HRP, γ-PGA-HEMA chains transformed into assemblies while incorporating HRP s simultaneously due to some weak interactions between the polymer chains and HRP enzymes, forming enzyme-loading HRP@γ-PGA-HEMA nanoparticles (HRP@PGH NPs). As shown in TEM image (Fig. 1B), HRP@PGH NPs exhibit a spherical shape with particle sizes distributing between 30 nm to 50 nm. The particle size observed from TEM image was smaller than the DLS result, which can be explains as follows. TEM characterization is usually conducted with dry samples under high vacuum, from which the morphologies of individual nanoparticles are presented in a dried state. DLS measures diffusion dynamics of the particle dispersions, thus providing information of an ensemble average hydrodynamic particle. Considering the high vacuum conditions of TEM and the hydrodynamic and electro-kinetic effects operative in DLS measurements, a discrepancy is often inevitable between TEM and DLS measurements. Therefore, the particle sizes provided by DLS and TEM is different and sometimes complementary (Ito et al., 2004). The discrepancy between TEM and DLS results can be more obvious when it comes to colloidal polymeric NPs, especially when the polymers are more solvophilic for chains extension in solvent. For polymeric NPs, the size determined by DLS is larger than that by TEM and AFM, which is due to the swollen structure of polymeric NPs in aqueous solution (DLS tests the size in the state that the polymer chains are in stretched states) (Chenglin et al., 2012). For pure γ-PGA-HEMA, the polymer chains are extended at high degree in water. For HRP@γ-PGA-HEMA, the interactions between HRP enzymes and γ-PGA-HEMA would drive γ-PGA-HEMA chains to contract, however, the polymer chains are still cannot be completely compacted together due to the solvent is good for γ-PGA-HEMA to stretch. Thus, much space exists between intermolecular chains in water and DLS gives the size results in this solvated state. However, the TEM image was taken in dry samples, which the polymer chains would shrink during the dehydration process. Therefore, the diameter from TEM characterization is smaller than DLS result. Similar discrepancy on the particle sizes of polymeric NPs by TEM and DLS have been widely reported and demonstrated (Chenglin et al., 2012; Huang et al., 2018; Luo et al., 2016). AFM results further confirmed the spherical nanostructure of the obtained HRP@PGH NPs (Fig. 1C). The well-distributed independent particles observed in TEM and AFM

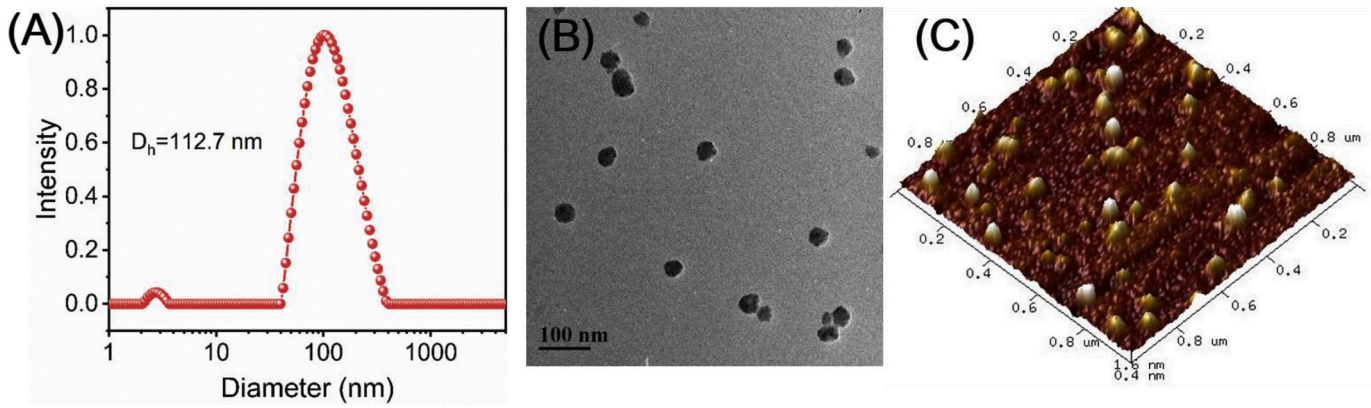

Fig. 1. Size and morphology of HRP@PGH NPs. (A) DLS plot, (B) TEM image and (C) AFM image of HRP@PGH NPs.

images provide strong evidence for the good dispersion stability of HRP@PGH NPs, which is because of the electrostatic repulsion interactions between these negatively charged HRP@PGH NPs. The nano size of enzyme-loaded polymeric NPs would afford high specific surface area which can contribute to the effective immobilization of enzyme molecules. In addition, the reaction path between the substrate and enzymes would be shortened when constructing bio-sensing interface.

To further certify the successful loading of HRP in HRP@PGH NPs, UV–visible (UV–vis) absorption spectra of pure HRP, γ-PGA-HEMA, and HRP@PGH NPs were recorded (Fig. S4A). In comparison to γ-PGA-HEMA, a new absorption peak at 403 nm appeared in the complex HRP@PGH NPs which coincides with the characteristic peak of native HRP (Zhao et al., 2016). The UV–vis results indicate the successful co-assembly of HRP and γ-PGA-HEMA. CD is a powerful tool for studying secondary protein structures (Jia et al., 2019; Xu et al., 2019b; Yang et al., 2019). To investigate the compatibility of γ-PGA-HEMA with encapsulated HRP further, the far-UV circular dichroism (CD) spectra of HRP and HRP@PGH NPs were performed in Fig. S4B. HRP@PGH NPs showed a similar CD spectrum to that of pure HRP, indicating that the original conformation of immobilized HRP molecules in HRP@PGH NPs was retained (Besharati Vineh et al., 2018). Overall, these CD results manifest that γ-PGA-HEMA macromolecules provide an appropriate micro-environment for HRP immobilization, which is beneficial to the preservation of HRP's biological activity without denaturation in HRP@PGH NPs composite.

3.3. Characterization of GO nanosheets

To characterize the structure of prepared GO nanosheets (GO NSs), Raman spectroscopy and FT-IR were used to confirm the successful synthesis of GO NSs with oxygen-bearing groups on the GO sheet surfaces (Fig. S5A and Fig. S5B). In addition, TEM and AFM images were used to characterize the surface morphologies of GO NSs, indicating the single layer topographical structure of GO NSs (ca. 1.05 nm thick) with lateral dimensions ranging from submicrometer to several micrometers (Figs. S5C–D and Fig. S6). The detailed characterizations of GO NSs can be found in the Supporting Information.

3.4. Interfacial properties of the biosensing films

To prepare bio-composite sensing film based on HRP@PGH NPs and GO NSs, electrophoretic deposition (EPD) was used to conduct the whole process due to its facile and effective nature. EPD is a convenient method widely used for manipulation and deposition of nanomaterials on substrates, which results in uniform film or coating for numerous applications from lab research to industrial production (Ahmad et al., 2018; Avcu et al., 2019). Recently, EPD of graphene-related materials has emerged as a productive approach for graphene based functional coatings. In particular, the co-deposition of nanoparticles or polymers alongside graphene or GO is essential for preparing composite films, which can introduce considerable flexibility and synergistic functionality (Diba et al., 2016; Ma et al., 2018).

Thanks to the negative charge of HRP@PGH NPs and GO NSs, it's highly expected that the 0D enzyme-loaded NPs can be co-deposited onto the surface of electrode simultaneously while proceeding the deposition of the 2D GO NSs process. As shown in Scheme 1B, the one-step EPD process was conducted in the mixed dispersion of HRP@PGH NPs and GO NSs for 120 s at a constant voltage of 1.5 V (*vs* SCE), generating the HRP@PGH/GO film on the electrode surface. To reduce GO NSs into graphene nanosheets (GNs) in the composite film, cyclic voltammogram (CV) was performed on the HRP@PGH/GO modified electrode in N_2 saturated PBS solution. As shown in Fig. S7, a large cathodic peak current at -1.3 V (*vs* SCE) was observed with an onset potential at approximately -0.4 V (*vs* SCE). The large cathodic peak is attributed to the electrochemical reduction of oxygen-containing groups on GO NSs surfaces (Mani et al., 2013; Wen et al., 2016). For subsequent cycles, the cathodic peak current showed a clear decrease, indicating the considerable and irreversible reduction of GO NSs. To fully reduce GO NSs, CV was performed for 15 cycles until no cathodic peak current can be observed, obtaining the composite HRP@PGH/GNSs bio-sensing film. FT-IR spectrometer and Raman spectroscopy (Fig. S8) were used to characterize the composite films before and after electrochemical reduction process, which verify the successful electrochemical reduction of GO NSs into GNSs in the composite film (detail information is shown in Supporting Information). The obtained GNSs in the composite film act as conducting nano-supports and nano-fillers for accelerating the electron transfer across the sensing bio-interface, which would enhance the response sensitivity toward substrates when applying the HRP@PGH/GNSs film as a bio-sensing platform.

The presence of HEMA units in γ-PGA-HEMA permits this biopolymer with photo-cross-linkable ability which would form cross-linked polymer network among neighboring polymer chains upon exposure to UV light. To demonstrate the effectiveness of photo-cross-linking, pure HRP@PGH NPs were deposited onto electrode surfaces using the EPD method. For comparison, surface topographies of HRP@PGH NPs modified electrodes without and with UV irradiation were characterized by SEM (Fig. S9A). As showed in Fig. S9A, HRP@PGH NPs formed uniform nanoparticles film with a rough topology on the electrode surface by EPD process. It is noteworthy that the enzyme-loaded NPs did not completely link together, which is likely to be due to polymer shrinkage during the naturally drying process (Luo et al., 2016). After UV irradiation, the nanostructured particles become linked with neighboring particles to a larger extent, forming a more continuous and compact particles film (Fig. S9B). To make a clearer observation from the SEM images, enlarged views of the SEM images of HRP@PGH NPs modified GCEs before and after UV irradiation were provided in Fig. S9a and Fig. S9b, respectively, which demonstrates the more compact surface structure of cross-linked HRP@PGH NPs film as a result of the photo-polymerization of HEMA units in the polymer chains. The SEM results reveal that photo-induced cross-linking had taken place across the whole film, which could improve the structural stability of hybrid NPs as well as the entire composite film.

For co-deposition of GO NSs and HRP@PGH NPs, the content of GO NS in the binary mixture plays a vital role in forming the final HRP@PGH/GNs bio-film. Therefore, the influence of GO NS concentration on the formation of composite bio-film was studied. SEM images (Fig. 2) reveal that the GO NSs and HRP@PGH NPs were simultaneously deposited onto electrode surfaces, resulting in the final 0D-2D HRP@PGH/GNSs composite film. With increasing GO NS concentrations for co-deposition, the surface topography of obtained composite film become much rougher resulting from the wrinkled feature of GNSs, which would greatly increase the specific surface area, providing more active sites for bio-sensing. However, when the GO NS concentration reached 0.2 mg mL^{-1}, the HRP@PGH/GNSs can no longer completely decorate most of the GNSs surfaces, resulting in "discrete NPs decorating corrugated NSs" morphology. CV technique was further employed to explore the electrochemical properties of the bio-sensing films derived from different GO NS concentrations. CV curves were recorded using $[Fe(CN)_6]^{3-/4-}$ as an electrochemical probe, which can reveal the kinetic barrier behaviors of the composite film across the probe and electrode interface. As shown in Fig. S10, the increase of GNSs in the composite film leads to enhanced redox peak current of the $[Fe(CN)_6]^{3-/4-}$ probe generally, which is in line with the morphological variations from SEM observations. CV results indicate that GNSs act as effective conductive nanofillers in the electrical improvement of the sensing film, which would speed up electron transporting between the recognition sites and the electrode. Considering that the loosely combined composite film at too high GNSs content may lead to low stability in aqueous environment, composite bio-sensing coating prepared at a GO NS concentration of 0.1 mg mL^{-1} were applied for biosensor fabrication and application.

To investigate the electrochemical behaviors of different electrodes, electrochemical impedance spectroscopy (EIS) and CV characterizations

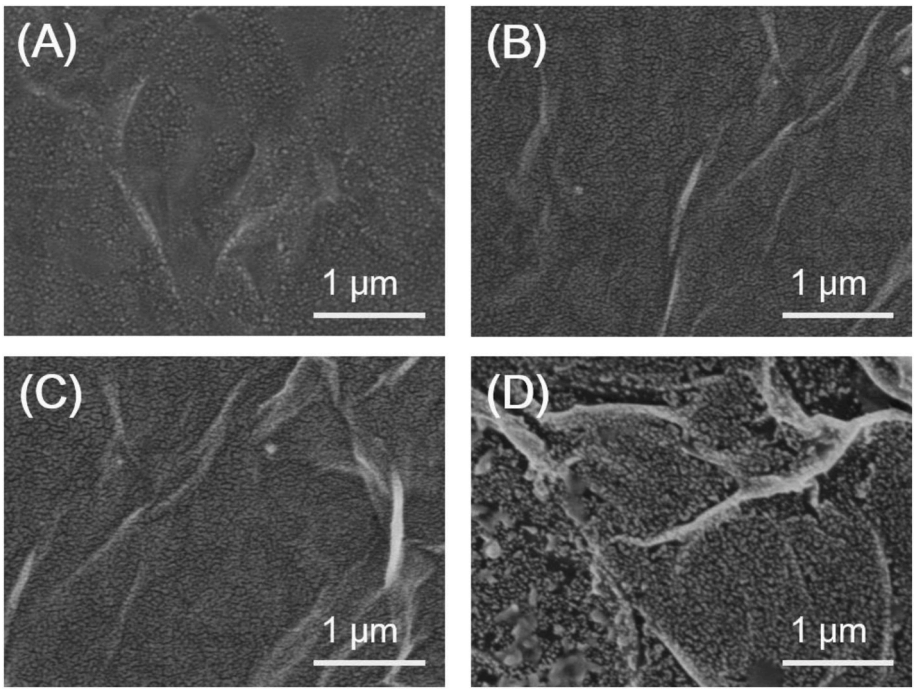

Fig. 2. SEM images of HRP@PGH/GNSs composite films on GCE surfaces prepared by electrophoretic co-deposition with different GO NS concentrations: (A) 0.02 mg mL^{-1}, (B) 0.05 mg mL^{-1}, (C) 0.1 mg mL^{-1}, and (D) 0.2 mg mL^{-1}.

were implemented (Fig. 3). The Nyquist plot typically contains two parts: a semicircular part at high frequency indicating electron transfers and a linear part at low frequency indicating diffusion phenomenon. The diameter of the semicircular part, considered as electron transfer resistance (R_{ct}), is a critical parameter to study the electron transmission at the material interface (Zhao et al., 2019). The corresponding impedance values were fitted according to the Randles equivalent circuit (inset of Fig. 3A), and were listed in Table S1. As exhibited in Fig. 3A, a linear Nyquist plot (plot a) can be seen for the bare electrode. In contrast, HRP@PGH NPs modified electrode shows a dramatic increase in electron transfer resistance with a R_{ct} value of ca. 5500 Ω (plot b), which is attributed the electrically inert nature of enzymes and the biopolymer. In plot c, the incorporation of GO NSs led to a remarkable decrease in R_{ct} value to ca. 2100 Ω, which could be due to the improved electrical conductivity from the GO NSs as well as the enlarged surface area. After electrochemical reduction of GO NSs into GNSs, the R_{ct} value decreased to ca. 1500 Ω as a result of the reduction oxygen-containing groups, indicating the successful conversion of GO NSs to GNSs (plot d). The CV curves in Fig. 3B illustrate the electrochemical behavior of different electrodes towards the redox probe. As shown in plot a, it exhibited a pair of reversible redox peaks on the bare GCE surface. The coverage of HRP@PGH NPs resulted in a significant decrement of the redox currents because the interface diffusion of the redox probe was hindered (plot b). By contrast, the redox currents increased in the presence of GO NSs in the sensing film (plot c). The further enhanced peak currents of the HRP@PGH/GNSs modified electrode verified the effectiveness of the GNSs in the electrical improvement of the bio-sensing film, which could be readily used in electrochemical bio-sensing.

3.5. Sensing performance

Hydrogen peroxide (H_2O_2) has been regarded as a short-term indicator of disease related problems in various fields, such as pharmaceuticals, industrials, fuel cells, and environmental protection (Liu et al., 2019). In human system, excessive H_2O_2 accumulation can cause a cytotoxic effect, resulting in some cell-related diseases (Su et al., 2017). To cope with these problems, exploiting reliable and efficient strategies for H_2O_2 monitoring is of significant importance. Enzymatic biosensors

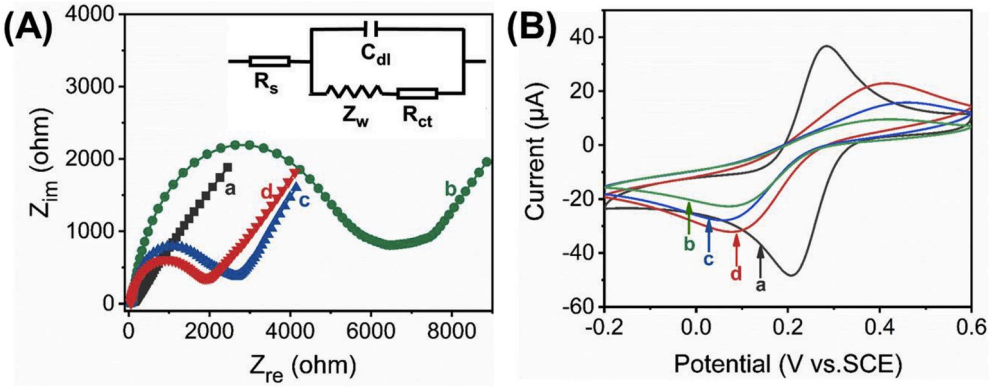

Fig. 3. (A) Nyquist plots and (B) CV curves of (a) bare GCE, (b) HRP@PGH NPs modified GCE, (c) HRP@PGH/GO NSs modified GCE and (d) HRP@PGH/GNSs modified electrode in 0.1 M KCl solution containing 5 mM $[Fe(CN)_6]^{3-/4-}$. Inset: the Randles equivalent circuit.

offer superior sensing performance than many traditional tools, which have shown the greatest potential for commercialization in real-life applications (Fan et al., 2015). For enzymatic H_2O_2 biosensors, HRP has been regarded as an optimal bio-catalytic enzyme for its high reliability, availability and low cost. (Liu et al., 2016).

For biosensor application, the bio-composite HRP@PGH/GNSs was applied as the sensing material for biosensor fabrication, and the electrochemical sensing performance towards hydrogen peroxide (H_2O_2) was demonstrated. The electrochemical behavior of the HRP@PGH/GNSs film based biosensor towards H_2O_2 was investigated by CV (Fig. S11A). As shown, due to the redox reaction of heme groups in HRP, a redox peak can be observed on the HRP@PGH/GNSs modified electrode in blank PBS solution. In the presence of H_2O_2, the response current at -0.7 V (*vs* SCE) showed a significant increase, indicating the bioactivity of immobilized HRP was maintained. Therefore, it could exhibit excellent electrocatalytic activity towards H_2O_2 reduction. In addition, to exclude the possibility of non-enzymatic reduction, CV curves of PGH NPs/GNSs/GCE and HRP@PGH NPs/GNSs/GCE in the same concentration of H_2O_2 were compared in Fig. S11B, which indicates the predominant enzyme catalysis reaction in the bio-sensing process. The electrocatalytic mechanism of the enzymatic biosensor towards H_2O_2 is presented in Equations (1)–(3) in Supporting Information (Nandini et al., 2013; Su et al., 2018).

3.5.1. *Calibration curve towards H_2O_2 detection*

The H_2O_2 detection performance of the HRP@PGH/GNSs sensor was explored by chronoamperometry under the optimized condition (the working potential was −0.7 V). Fig. 4A illustrates the steady-state-current responses upon successive injection of H_2O_2 into PBS (0.1 M, pH 7.0). The sensor exhibited a sensitive and rapid response to H_2O_2 with very short response time (within 3 s). The fast response is mainly due to the hierarchical 0D NPs decorating 2D nanosheet structure of the bio-sensing film, which permits the rapid H_2O_2 diffusion through the film and the synergistic catalytic effect toward H_2O_2 (Zeng et al., 2010). Fig. 4B shows the calibration curve of the electrocatalytic current of the enzymatic biosensor against H_2O_2 concentration, in which a well-defined linear relationship between the response current and H_2O_2 concentration in the range from 1.0 μM to 340 μM was observed. The linear equation can be expressed as I (μA) = 1.4201 + 0.01604 C_{H2O2} (μM) (R^2 = 0.998) with a low detection limit (LOD) of 0.27 μM (S/N = 3). The analytical performance of our biosensor was compared with some previously reported H_2O_2 enzymatic biosensors (Table S2). As displayed, compared to other nanomaterials based enzymatic biosensors, our biosensor shows satisfactorily wide linear detection range with a lower LOD of H_2O_2. Though some graphene-containing composites based biosensors in Table S2 have wider linear detection ranges, these composites used in biosensors often incorporate other noble-metal nanoparticles (like gold or silver nanoparticles) besides polymers and graphene, making the preparation process of the sensing systems more intricate at higher cost. However, we can also learn lessons from other sensing composites which could help to widen the detection range of the developed sensor in our future work. For example, some electrically active units (such as carbazole and ferrocene units) could be incorporated in the polymer chains, or polymer/metal hybrid NPs could also be in-situ prepared which could combine with 2D graphene nanomaterials for enhanced synergistic effects for bio-sensing. On the whole, the comparison in sensing performance demonstrate the desirable sensing performance of our hierarchical 0D/2D HRP@PGH/GNSs composite

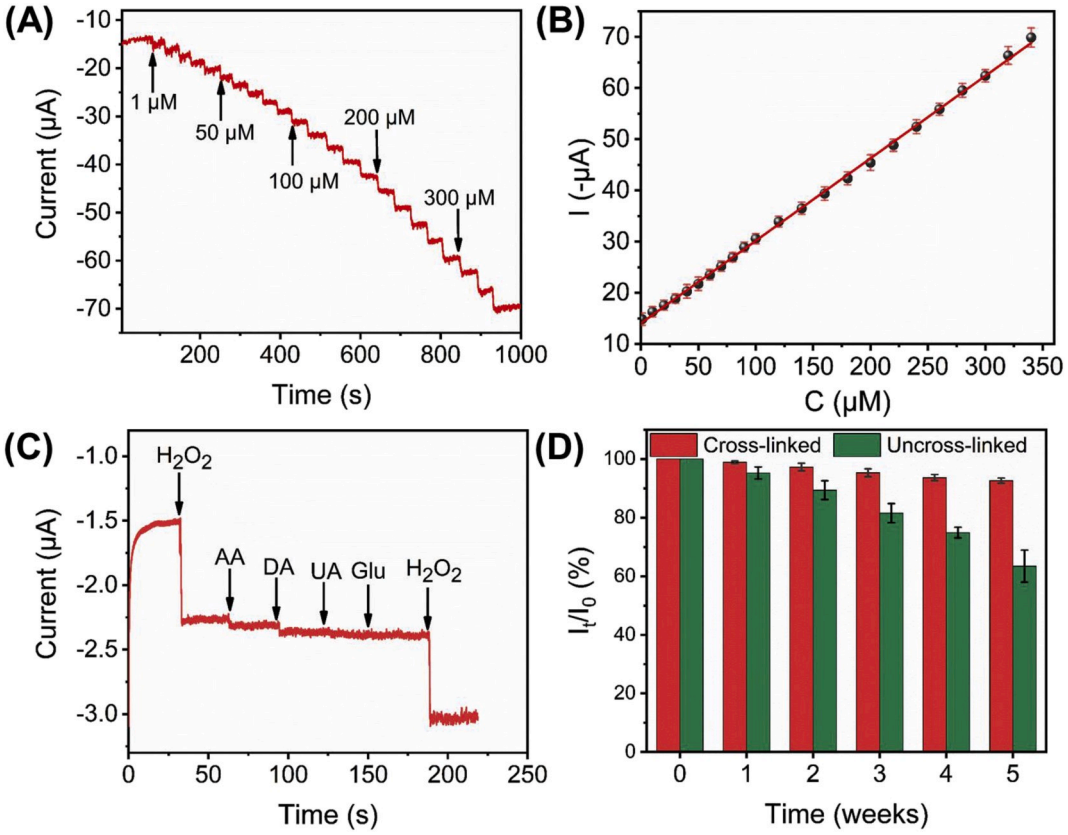

Fig. 4. (A) Amperometric response of HRP@PGH/GNSs/GCE on successively adding H_2O_2 to 0.1 M PBS (pH 7.0), working potential: −0.7 V (*vs.* SCE). (B) Calibration plot of current against H_2O_2 concentration (Error bar = ± RSD, n = 3). (C) Amperometric response of HRP@PGH/GNSs/GCE on successively adding 0.05 mM H_2O_2 and the interfering species of 0.5 mM AA, 0.5 mM DA, 0.5 mM UA, and 0.5 mM Glu in 0.1 M PBS. (D) Stability tests of the two biosensors based on photo-cross-linked and uncross-linked HRP@PGH/GNSs composite films toward 0.05 mM H_2O_2 over 5 weeks. I_t/I_0 (%) is the retention rate of amperometric current after t days of storage.

film based enzymatic biosensor for H_2O_2 determination.

In addition, the analytical performances of biosensors based on HRP-GNSs/GCE, HRP@PGH NPs/GCE, HRP@PGH/GNSs/GCE towards H_2O_2 detection were investigated and compared (Fig. S12). As shown in Fig. S12A, for the HRP-GNSs modified electrode without polymer support (curve a), the current response sensitively increased with increasing the H_2O_2 concentration (sensitivity can be reflected by the slope). However, the increasement in response current became irregular after several addition of H_2O_2, which is resulted from the enzyme fell off the GNSs surfaces due to the weak interactions between enzymes and GNSs. For the HRP@PGH NPs modified electrode without GNSs (curve b), though the response current kept increasing on successive addition of H_2O_2, the sensitivity of the biosensor's response towards is H_2O_2 is too weak which can hardly be distinguished from the background noise (Fig. S12B). The low sensitivity of HRP@PGH NPs modified electrode can be ascribed to the poor conductive property of γ-PGA-HEMA polymer, which limits the electron transmission in the bio-sensing interface. In contrast, the HRP@PGH/GNSs/GCE based biosensor (curve c) exhibited linear current responses on successive addition of H_2O_2 compared to HRP-GNSs/GCE, and much higher sensitivity than HRP@PGH NPs/GCE. The excellent performance of this developed biosensor is resulted from the material nature and special architecture of the HRP@PGH/GNSs bio-film. The functionalized γ-PGA-HEMA provide high biocompatibility for preserving enzyme activities, while the nanosized HRP@PGH NPs offers large surface area for high enzyme loading with enhanced stability. In addition, the graphene nanosheets as fillers and supports provide high conductivity for the rapid response toward H_2O_2 detection. Meanwhile, a synergistic catalytic effect caused by this multiple-component system plays a significant role to improve the whole performance. The combination of the 0D HRP@PGH NPs and graphene NSs as a whole offers excellent sensitivity and rapid response for the fabrication of HRP@PGH/GNSs sensing platform.

3.5.2. Anti-interference performance

A key character of an enzyme biosensor is its specificity for target analyte while discriminating other foreign species in a complex solution system. To investigate the anti-interference ability of the HRP@PGH/GNSs biosensor, some interfering species with a same concentration of 0.5 mM, including ascorbic acid (AA), dopamine (DA), uric acid (UA) and glucose (Glu) were successively used as interferents in the amperometric H_2O_2 (0.05 mM) detection process. As displayed in Fig. 4C, interferents at much higher concentration (10 fold) than H_2O_2 showed negligible responses in comparison to H_2O_2, demonstrating the high anti-interference ability of the developed biosensor. The anti-interference result evidenced that the HRP@PGH/GNSs based biosensor could be potentially applied in a complex physiological environment for H_2O_2 determination.

3.5.3. Reproducibility and stability

To assess the reproducibility, five independent H_2O_2 biosensors were fabricated under the same condition based on the bio-composite HRP@PGH/GNSs film. Under identical test condition, the response currents of the five biosensors to 50 μM H_2O_2 were recorded and shown in Fig. S13. The five biosensors exhibited a relative standard value of 2.80% at the same H_2O_2 concentration, illustrating excellent reproducibility of the HRP@PGH/GNSs based enzymatic biosensor. Stability is a crucial factor for workable electrochemical sensors and especially for biosensors, which has a strong influence on the practical applicability of biosensors (Ren et al., 2017b). The stability of the HRP@PGH/GNSs based biosensor was evaluated by testing the biosensor's response currents every seven days over five weeks by storing the biosensor at 4 °C. To illustrate the influence of photo-cross-linking on the sensing stability, the response currents of HRP@PGH/GNSs based biosensors with and without photo-cross-linking over time were measured and compared. As displayed in Fig. 4D, the uncross-linked HRP@PGH/GNSs film based biosensor deteriorated its current response toward H_2O_2 by a great extent over time and retained only 63.46% of the initial value after 35 days, which could be resulted from enzyme leaking out of the bio-composite film after exposing to aqueous solution for several times. In contrast, a high current retention value of 92.62% of the photo-cross-linked biosensor was observed after five weeks, demonstrating that the biosensor with photo-cross-linking had enhanced sensing stability. Photo-cross-linking can improve the structural stability of the bio-composite film by constructing interlinked network, thus contributing to high resistance to solution environment (Xu et al., 2018). What's more, γ-PGA-HEMA could offer a favorable microenvironment for preserving the biological activity of the loaded enzymes in the polymer matrix. As a consequence, the developed HRP@PGH/GNSs based biosensor exhibited high stability.

3.5.4. Real application in human serum

To prove the biosensor's practicability in real samples, the fabricated HRP@PGH/GNSs biosensor was used to determine H_2O_2 content in human serum donated from a local hospital following the standard addition method (Mohammadniaei et al., 2018). Prior to the test, serum samples were diluted 100-fold with PBS buffer (pH 7.0). H_2O_2 from serum samples was measured by spiking a known content of H_2O_2 and calculating the content according to the linear detection equation using the recorded current responses. As displayed in Table 1, the detected H_2O_2 contents were in good line with spiked values with acceptable recoveries from 96.80% to 104.46%, illustrating that the developed biosensor is reliable to be practically used in biomedical fields.

4. Conclusions

In summary, this work developed an effective strategy for constructing robust enzymatic bio-sensing platform based on one-step electrodeposition of 0D enzyme-loaded bio-polymeric nanoparticles (NPs) with 2D graphene oxide nanosheets as conductive nanosupports. The enzymatic biosensor exhibited excellent sensing performance which is a synergistic result from both the design of materials and the hierarchically 0D-2D nanostructure. For material, the photo-cross-linkable polypeptide γ-PGA-HEMA not only provided a biocompatible microenvironment to favor HRP enzymes' bio-activity, but also enhanced the structural stability of the bio-composite sensing film as a result of photo-induced cross-linking. And the conductive GNSs could effectively accelerate electrons travelling across the sensing interface, thus improved of the biosensor's sensitivity. For the nanostructure, the 0D enzyme-polymer NPs decorating 2D NSs bio-composite film had high active surface area, giving rise to more recognition sites and favored the mass transfer process. As a result, the enzymatic biosensor showed high sensitivity, high selectivity and enhanced stability. Significantly, the biosensor was applied in real human blood serum samples, which demonstrates reliable applicability in real complex biological environment. As a proof-of concept strategy, the developed hierarchical 0D-2D composite film as a novel bio-sensing platform synergistically takes the independent advantages of both the polymer nanoparticles and conductive carbon nanosheets. We believe this pioneering work would provide referential lessons and useful inspiration for new generation of bio-sensing devices.

Table 1
Recovery test of H_2O_2 in blood serum samples.

Samples		Spiked (μM)	Detected (μM)	Recovery (%)	RSD(n = 3) (%)
Blood serum	1	10	9.68	96.80	3.04
	2	50	52.17	104.34	2.39
	3	100	104.46	104.46	2.83

Declaration of competing interest

The authors declare that they have no known competing financial interests or personal relationships that could have appeared to influence the work reported in this paper.

CRediT authorship contribution statement

Sheng Xu: Conceptualization, Methodology, Formal analysis, Investigation, Writing - original draft, Data curation, Visualization. **Yayuan Liu:** Investigation, Data curation, Visualization. **Wei Zhao:** Formal analysis, Data curation, Validation. **Qian Wu:** Investigation, Data curation, Validation. **Yanru Chen:** Investigation, Visualization. **Xuewen Huang:** Investigation. **Zhijian Sun:** Visualization. **Ye Zhu:** Writing - review & editing, Validation, Validation, Project administration, Funding acquisition. **Xiaoya Liu:** Methodology, Writing - review & editing, Validation, Project administration, Supervision, Funding acquisition.

Acknowledgments

We are grateful to the funding from National Natural Science Foundation of China (51573073 and 51803079). S. X. greatly appreciates the technical help from many lovely teachers like Haiyan Zhu, Junkang Liu, Yao Gu, and et al. in Jiangnan University during his Ph.D career. S. X. is also thankful to Dr. Ching-Ping Wong in Georgia Institute and Technology for his valuable suggestions in research and life.

Appendix A. Supplementary data

Supplementary data to this article can be found online at https://doi.org/10.1016/j.bios.2020.112134.

References

Ahmad, R., Wolfbeis, O.S., Hahn, Y.-B., Alshareef, H.N., Torsi, L., Salama, K.N., 2018. Deposition of nanomaterials: a crucial step in biosensor fabrication. Mater. Today Commun. 17, 289–321.

Avcu, E., Baştan, F.E., Abdullah, H.Z., Rehman, M.A.U., Avcu, Y.Y., Boccaccini, A.R., 2019. Electrophoretic deposition of chitosan-based composite coatings for biomedical applications: a review. Prog. Mater. Sci. 103, 69–108.

Besharati Vineh, M., Saboury, A.A., Poostchi, A.A., Rashidi, A.M., Parivar, K., 2018. Stability and activity improvement of horseradish peroxidase by covalent immobilization on functionalized reduced graphene oxide and biodegradation of high phenol concentration. Int. J. Biol. Macromol. 106, 1314–1322.

Chenglin, Y., Yiqun, Y., Ye, Z., Na, L., Xiaoya, L., Jing, L., Ming, J., 2012. Self-assembly and emulsification of poly{[styrene-alt-maleic acid]-co-[styrene-alt-(N -3,4-dihydroxyphenylethyl-maleamic acid)]}. Langmuir 28, 9211–9222.

Das, P., Das, M., Chinnadayyala, S.R., Singha, I.M., Goswami, P., 2016. Recent advances on developing 3rd generation enzyme electrode for biosensor applications. Biosens. Bioelectron. 79, 386–397.

Diba, M., Fam, D.W.H., Boccaccini, A.R., Shaffer, M.S.P., 2016. Electrophoretic deposition of graphene-related materials: a review of the fundamentals. Prog. Mater. Sci. 82, 83–117.

Fan, Z., Lin, Q., Gong, P., Liu, B., Wang, J., Yang, S., 2015. A new enzymatic immobilization carrier based on graphene capsule for hydrogen peroxide biosensors. Electrochim. Acta 151, 186–194.

Gerard, M., Chaubey, A., Malhotra, B.D., 2002. Application of conducting polymers to biosensors. Biosens. Bioelectron. 17, 345–359.

Huang, J., Tong, J., Luo, J., Zhu, Y., Gu, Y., Liu, X., 2018. Green synthesis of water-compatible fluorescent molecularly imprinted polymeric nanoparticles for efficient detection of paracetamol. ACS Sustain. Chem. Eng. 6, 9760–9770.

Ito, T., Sun, L., Bevan, M.A., Crooks, R.M., 2004. Comparison of nanoparticle size and electrophoretic mobility measurements using a carbon-nanotube-based coulter counter, dynamic light scattering, transmission electron microscopy, and phase analysis light scattering. Langmuir 20, 6940–6945.

Jia, Y., Yang, L., Feng, Ruiqing, Ma, H., Fan, D., Yan, T., Feng, Rui, Du, B., Wei, Q., 2019. $MnCO_3$ as a new electrochemiluminescence emitter for ultrasensitive bioanalysis of β-Amyloid 1-42 oligomers based on site-directed immobilization of antibody. ACS Appl. Mater. Interfaces 11, 7157–7163.

Justino, C.I.L., Gomes, A.R., Freitas, A.C., Duarte, A.C., Rocha-Santos, T.A.P., 2017. Graphene based sensors and biosensors. TrAC Trends Anal. Chem. 91, 53–66.

Lee, D., Lee, J., Kim, J., Kim, J., Na, H.B., Kim, B., Shin, C.-H., Kwak, J.H., Dohnalkova, A., Grate, J.W., Hyeon, T., Kim, H.-S., 2005. Simple fabrication of a highly sensitive and fast glucose biosensor using enzymes immobilized in mesocellular carbon foam. Adv. Mater. 17, 2828–2833.

Liu, F., Piao, Y., Choi, K.S., Seo, T.S., 2012. Fabrication of free-standing graphene composite films as electrochemical biosensors. Carbon 50, 123–133.

Liu, H., Guo, K., Duan, C., Chen, X., Zhu, Z., 2016. A novel biosensor based on the direct electrochemistry of horseradish peroxidase immobilized in the three-dimensional flower-like Bi_2WO_6 microspheres. Mater. Sci. Eng. C 64, 243–248.

Liu, Wenping, Pan, H., Liu, C., Su, C., Liu, Wenbo, Wang, K., Jiang, J., 2019. Ultrathin phthalocyanine-conjugated polymer nanosheet-based electrochemical platform for accurately detecting H_2O_2 in real time. ACS Appl. Mater. Interfaces 11, 11466–11473.

Lu, D., Cardiel, J., Cao, G., Shen, A.Q., 2010. Nanoporous scaffold with immobilized enzymes during flow-induced gelation for sensitive H_2O_2 biosensing. Adv. Mater. 22, 2809–2813.

Luo, J., Ma, Q., Wei, W., Zhu, Y., Liu, R., Liu, X., 2016. Synthesis of water-dispersible molecularly imprinted electroactive nanoparticles for the sensitive and selective paracetamol detection. ACS Appl. Mater. Interfaces 8, 21028–21038.

Ma, Y., Han, J., Wang, M., Chen, X., Jia, S., 2018. Electrophoretic deposition of graphene-based materials: a review of materials and their applications. J. Materiomics 4, 108–120.

Mani, V., Devadas, B., Chen, S.-M., 2013. Direct electrochemistry of glucose oxidase at electrochemically reduced graphene oxide-multiwalled carbon nanotubes hybrid material modified electrode for glucose biosensor. Biosens. Bioelectron. 41, 309–315.

Mohammadniaei, M., Yoon, J., Lee, T., Bharate, B.G., Jo, J., Lee, D., Choi, J.-W., 2018. Electrochemical biosensor composed of silver ion-mediated dsDNA on Au-encapsulated Bi_2Se_3 nanoparticles for the detection of H_2O_2 released from breast cancer cells. Small 14, 1703970.

Montheard, J.-P., Chatzopoulos, M., Chappard, D., 1992. 2-Hydroxyethyl Methacrylate (HEMA): chemical properties and applications in biomedical fields. J. Macromol. Sci. Polym. Rev. 32, 1–34.

Nandini, S., Nalini, S., Manjunatha, R., Shanmugam, S., Melo, J.S., Suresh, G.S., 2013. Electrochemical biosensor for the selective determination of hydrogen peroxide based on the co-deposition of palladium, horseradish peroxidase on functionalized-graphene modified graphite electrode as composite. J. Electroanal. Chem. 689, 233–242.

Putzbach, W., Ronkainen, N., Putzbach, W., Ronkainen, N.J., 2013. Immobilization techniques in the fabrication of nanomaterial-based electrochemical biosensors: a review. Sensors 13, 4811–4840.

Ren, X., Ma, H., Zhang, T., Zhang, Y., Yan, T., Du, B., Wei, Q., 2017a. Sulfur-doped graphene-based immunological biosensing platform for multianalysis of cancer biomarkers. ACS Appl. Mater. Interfaces 9, 37637–37644.

Ren, X., Yan, J., Wu, D., Wei, Q., Wan, Y., 2017b. Nanobody-based apolipoprotein e immunosensor for point-of-care testing. ACS Sens. 2, 1267–1271.

Su, S., Han, X., Lu, Z., Liu, W., Zhu, D., Chao, J., Fan, C., Wang, Lihua, Song, S., Weng, L., Wang, Lianhui, 2017. Facile synthesis of a MoS_2–prussian blue nanocube nanohybrid-based electrochemical sensing platform for hydrogen peroxide and carcinoembryonic antigen detection. ACS Appl. Mater. Interfaces 9, 12773–12781.

Su, Y., Zhou, X., Long, Y., Li, W., 2018. Immobilization of horseradish peroxidase on amino-functionalized carbon dots for the sensitive detection of hydrogen peroxide. Microchim. Acta 185, 114.

Sung, M.H., Park, C., Kim, C.J., Poo, H., Soda, K., Ashiuchi, M., 2005. Natural and edible biopolymer poly-γ-glutamic acid: synthesis, production, and applications. Chem. Rec. 5, 352–366.

Turner, A.P.F., 2013. Biosensors: sense and sensibility. Chem. Soc. Rev. 42, 3184–3196.

Veitch, N.C., 2004. Horseradish peroxidase: a modern view of a classic enzyme. Phytochemistry 65, 249–259.

Wen, Y., Wen, W., Zhang, X., Wang, S., 2016. Highly sensitive amperometric biosensor based on electrochemically-reduced graphene oxide-chitosan/hemoglobin nanocomposite for nitromethane determination. Biosens. Bioelectron. 79, 894–900.

Xu, S., Huang, X., Chen, Y., Liu, Y., Zhao, W., Sun, Z., Zhu, Y., Liu, X., Wong, C.-P., 2019a. Silver nanoparticle-enzyme composite films for hydrogen peroxide detection. ACS Appl. Nano Mater. 2, 5910–5921.

Xu, S., Lin, G., Zhao, W., Wu, Q., Luo, J., Wei, W., Liu, X., Zhu, Y., 2018. Necklace-like molecularly imprinted nanohybrids based on polymeric nanoparticles decorated multiwalled carbon nanotubes for highly sensitive and selective melamine detection. ACS Appl. Mater. Interfaces 10, 24850–24859.

Xu, S., Zhang, R., Zhao, W., Zhu, Y., Wei, W., Liu, X., Luo, J., 2017. Self-assembled polymeric nanoparticles film stabilizing gold nanoparticles as a versatile platform for ultrasensitive detection of carcino-embryonic antigen. Biosens. Bioelectron. 92, 570–576.

Xu, S., Zhang, Y., Zhu, Y., Wu, J., Li, K., Lin, G., Li, X., Liu, R., Liu, X., Wong, C.-P., 2019b. Facile one-step fabrication of glucose oxidase loaded polymeric nanoparticles decorating MWCNTs for constructing glucose biosensing platform: structure matters. Biosens. Bioelectron. 135, 153–159.

Yang, H., 2012. Enzyme-based ultrasensitive electrochemical biosensors. Curr. Opin. Chem. Biol. 16, 422–428.

Yang, L., Fan, D., Zhang, Y., Ding, C., Wu, D., Wei, Q., Ju, H., 2019. Ferritin-based electrochemiluminescence nanosurface energy transfer system for procalcitonin detection using HWRGWVC heptapeptide for site-oriented antibody immobilization. Anal. Chem. 91, 7145–7152.

Zeng, Q., Cheng, J., Tang, L., Liu, X., Liu, Y., Li, J., Jiang, J., 2010. Self-assembled graphene-enzyme hierarchical nanostructures for electrochemical biosensing. Adv. Funct. Mater. 20, 3366–3372.

Zhang, R., Chen, W., 2017. Recent advances in graphene-based nanomaterials for fabricating electrochemical hydrogen peroxide sensors. Biosens. Bioelectron. 89, 249–268.
Zhao, W., Li, B., Xu, S., Huang, X., Luo, J., Zhu, Y., Liu, X., 2019. Electrochemical protein recognition based on macromolecular self-assembly of molecularly imprinted polymer: a new strategy to mimic antibody for label-free biosensing. J. Mater. Chem. B 7, 2311–2319.
Zhao, Y., Zheng, Y., Kong, R., Xia, L., Qu, F., 2016. Ultrasensitive electrochemical immunosensor based on horseradish peroxidase (HRP)-loaded silica-poly(acrylic acid) brushes for protein biomarker detection. Biosens. Bioelectron. 75, 383–388.
Zhu, C., Yang, G., Li, H., Du, D., Lin, Y., 2015. Electrochemical sensors and biosensors based on nanomaterials and nanostructures. Anal. Chem. 87, 230–249.